

GNSS multipath error in the context of the reliability of companion robots

Karolina KRZYKOWSKA-PIOTROWSKA¹, Emilia GRABKA¹, Ewa DUDEK¹,
 Adam ROSIŃSKI¹*, and Kamil MACIUK²

¹ Warsaw University of Technology, Faculty of Transport, ul. Koszykowa 75, 00-662 Warsaw, Poland

² AGH University of Krakow, ul. Mickiewicza 30, 30-059 Kraków, Poland

Abstract. A companion robot is capable of performing a variety of activities and thus supporting the elderly and people with disabilities. It should be able to overcome obstacles on its own, respond to what is happening around it in real time, and communicate with its surroundings. It is particularly important to pay attention to these issues, as a companion robot is likely to become a participant in traffic. The research aims to develop a mathematical model that considers the use of two navigation solutions in the companion robot. Thanks to this, it will be possible to use the obtained mathematical relationships to compare various types of navigation and make a rational choice, enabling the implementation of the assumed activities in a specific external environment. What is new in this paper is the analysis of several navigation methods and the presentation of research conducted in real time using an actual robot.

Keywords: companion robot; reliability; operation; navigation.

1. INTRODUCTION

According to demographic data, the average human life expectancy is increasing worldwide. This means that the populations of individual highly developed countries are growing old. It is expected that the proportion of elderly people in society will significantly increase over the next several years. The outbreak of the coronavirus pandemic in 2019 highlighted the need for the implementation of new technological solutions for everyday assistance for the elderly and people with disabilities. Many innovations enhance everyday life, including the option of utilizing a companion robot to deal with global changes [1]. Nowadays, technology has advanced to the point where devices are capable of assisting the elderly and people with disabilities. The companion robot software enables it to perform a range of operations, starting from simply reminding one to take their medication, dressing them appropriately for the occasion, doing planned shopping, reading a timetable, or keeping humans company [2]. It also provides blind people with enormous assistance in moving around outside. A robot could replace a guide dog and, in addition, could describe the surroundings and assist when communicating with the outside world [3].

Considerations concerning companion robots are realised using different approaches, depending on the type and scope of scientific and implementation research. One of the more frequently considered approaches to companion robots is the issue of ensuring an appropriate level of security in the transmission

of information between the robot and its surroundings [4]. This is because a companion robot is a servant robot that is used for work that is time-consuming or requires a lot of physical or intellectual effort from humans. Models of autonomous robots for industrial purposes are rather well-developed. Designing such a robot is significantly facilitated because it moves in a well-characterised space, and the changes occurring in it are not dynamic.

A companion robot is capable of performing a variety of activities and thus supporting the elderly and people with disabilities. It is therefore required that the robot move in a diverse environment, primarily urban [5]. For this reason, a companion robot is very often designed and constructed to be humanoid so that it can perform its owner's tasks as simply and efficiently as possible.

A companion robot should be able to overcome obstacles on its own, respond to what is happening around it in real time, and communicate with its surroundings. It is particularly important to pay attention to these issues, as the robot is likely to become a participant in traffic [6]. This makes the issue of determining its position incredibly important. Not only does the correctness of this operation depend on the navigation solution applied to the companion robot but also on reliability and operational issues concerning the devices performing localisation functions. The research aims to develop a mathematical model that considers the use of two navigation solutions in the companion robot. Thanks to this, it will be possible to use the obtained mathematical relationships to compare various types of solutions used in the companion robot in terms of navigation and make a rational choice, facilitating the implementation of the assumed activities in a specific external environment. The above issues are considered in this paper. Its novelty is the presentation of research conducted in real time, using an actual robot.

*e-mail: adam.rosinski@pw.edu.pl

Manuscript submitted 2023-09-13, revised 2024-02-27, initially accepted for publication 2024-02-28, published in May 2024.

2. COMPANION ROBOT NAVIGATION

To properly perform the assigned tasks, the companion robot requires its position to be determined. Various navigation solutions can be applied for this purpose. A commonly used approach is the LIDAR-based technique which allows e.g. obstacles to be avoided and land to be mapped. An interesting proposal is the possibility of determining the position using satellite navigation systems GNSS (*Global Navigation Satellite Systems*), including the USA's GPS (*Global Positioning System*), the European system Galileo, Russia's system GLONASS (Russian: *Global'naya navigatsionnaya sputnikovaya sistema*), and the China's system BeiDou [7]. Such a solution would require a GNSS receiver to be installed inside (on the body of) the companion robot. The receiver receives signals from satellites placed in specific orbits, and the location of the companion robot is calculated based on them. The robot software then allows it to move along a designated route, thanks to the designated coordinates. In addition, the robot would have sensors installed to enable it to avoid possible obstacles while moving along the designated route [8].

An alternative to navigation using GNSS systems is the solution using the TDoA (*time difference of arrival*) method which involves the periodic emission of a signal. The signal is detected by receivers that are placed in fixed locations. When a large group of receivers detects the same signal, the location of the target can be inferred from the differences between detection times. The accuracy of this method is approximately 30 cm. It is not affected by as many errors as navigation using a GNSS signal is [9], but it has a much shorter range and requires appropriate adaptation to the environment [10].

Table 1 presents the advantages and disadvantages of particular navigation solutions that can be used in the companion robot.

Table 1

Advantages and disadvantages of navigation solutions in a companion robot

Criteria	LIDAR	GNSS	TDoA
Range	++	+++	+
Accuracy of location outside buildings	++	++	+
Accuracy of location inside buildings	+++	+	+++
Cost	+	++	+++
Environmental adaptation requirements	+++	+++	+

It can be seen that the LIDAR technique gives the best results in terms of positioning accuracy and adaptation in a diverse environment. GNSS works best in terms of navigation range and wide availability. In turn, TDoA is best when available inside buildings and is the most cost-efficient solution.

3. ASSESSMENT OF THE COMPANION ROBOT NAVIGATION IN THE CONTEXT OF GNSS SIGNAL MULTIPATH PROPAGATION

When analysing the issue of the assessment of the accuracy of the determined companion robot position, it can be concluded that the most significant factors that cause errors in navigation and positioning include the location of the satellites in relation to the receiver and the level of land urbanisation, and the terrain. An unfavourable location of the satellites results in the signal being reflected from various surfaces. The consequence of this is the multipath propagation of the signal, as a reflected signal reaching the receiver antenna travels a longer distance. Therefore, the position coordinates calculated by the receiver based on the signals received from the satellites may differ from the actual ones. A signal is most often reflected from flat surfaces and in locations where land is built up on all sides. It can be therefore assumed that the signal will be most disturbed among tall glass buildings and the least disturbed in open urban spaces. To verify the hypothesis about the impact of the environment and terrain on errors in navigation and positioning, i.e. the so-called multipath errors, and to determine the possible impact of these errors on the functioning of the companion robot, measurements were conducted in specific areas of the city of Warsaw.

The measurements were taken using a low-cost receiver with an antenna by UBLOX (thus simulating the movement of a companion robot). The data was recorded using a laptop computer with the U-CENTER software installed. All measurements were collated using images from maps from the website www.geoforum.pl and Google Maps and trajectory drawings from a tab in the RTKlib library attached to the U-CENTER program. The measurements were taken at seven locations in Warsaw (Table 2). For each location, a description is attached, showing the route along which the measurements took place.

To obtain the relevant data and determine the multipath error value, the coordinates of the measurement points for each measurement in the WGS 84 format were read out from the RTK Plot program. The program has the "show track point" option which enables the precise acquisition of this data. Once the data was acquired in this format, it was converted into coordinates in a two-dimensional system in the unit [m].

To determine the error magnitude, the actual route taken during the measurements was recreated. On this basis, the coordinates of the points through which the route passed were determined on the assumption that the robot taking measurements was travelling along straight lines. This was conducted using a reading of coordinates from the portal www.geoforum.pl.

Once the data was collected and converted into coordinates in the appropriate system, the hypothetical trajectories were compiled in the diagrams along with the measured data. This article includes two measurement results (measurements 1 and 6) which in the authors' opinion best illustrate the issue of assessing the correctness of determination of the companion robot location in the context of GNSS signal multipath propagation.

Table 2
Measurement location descriptions

Measurement	Location – Warsaw
1	Icchoka Leiba Pereca Street → Jana Pawła II Avenue → ONZ Roundabout → Prosta Street → Żelazna Street → Pereca Street
2	A section in the Mokotów Field via an alley leading to Żwirki and Wigury Street, near Sakura Park and the beach volleyball court → further along the entire length of the barbecue area
3	Measurement in the green areas among the student hostels located near the Gabriela Narutowicza Square
4	Measurement in the same location as measurement 3 but around the complex of student hostels: Uniwersytecka Street → Mochnickiego Street → Grójecka Street → Gabriela Narutowicza Square → Uniwersytecka Street
5	A section leading from the Zawisza Square near the Warszawa Główna Railway Station, along Towarowa Street, to the Daszyńskiego Roundabout
6	A section leading through Prosta Street on one side → change in direction and return along the same street on the other side → Wronia Street → Łucka Street → a passage between two office buildings, Frontex and BNP Paribas Security Services towards the Europejski Square → a passage between the Venturilo office building and the Samsung office building → a section of Towarowa Street to the bus stop
7	A section from Łucka Street to Prosta Street, between two office buildings: Generation Y and Centrum Medicover

Measurement 1

Figure 1 shows the measurement results recorded along the following route: Icchoka Leiba Pereca Street → Jana Pawła II Avenue → ONZ Roundabout → Prosta Street → Żelazna Street → Pereca Street. The Mennica Legacy Tower office building is specific, as it comprises a 140-metre-tall tower and a 43-metre Western Building. There are lower buildings around it, but the site is still built up on all sides. The first section of Icchoka Leiba Pereca Street is narrow, and the satellites are often found beyond the horizon. Another section towards the ONZ Roundabout is a more open space.

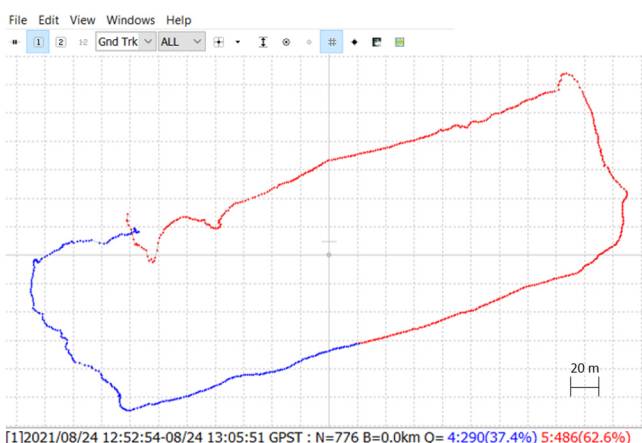


Fig. 1. The visualisation of the route course travelled during measurement No. 1 based on Google Maps [own study]

In the part shown in the diagram, the most crucial point is the place where the horizon is obscured by tall buildings. When comparing the measurement trajectory and the representation of the actual route, it can be seen that this is where the signal distortion occurs. The trajectory is different from that in reality, as on the last section of the travelled route, i.e. from the side

of Żelazna Street. On the remaining sections of the route, no major trajectory changes usually occurred. In general, it was assumed that the measurement was taken along a straight route on the pavement. The width of the pavement was two metres at the most. Therefore, it is recommended to accept such a level of error. Although the diagram indicates an error of over 40 m at a certain point, it should be noted that this could be due to receiver or data readout errors. Therefore, a difference of just a few meters may still be possible, having compensated for these errors.

Measurement 6

Figures 2 and 3 show the results of measurements recorded according to the route marked as 6 in Table 2. The measurement was taken among the tallest buildings in the centre of Warsaw. This shows very well how a signal can be disturbed in an urban environment as the buildings located along Prosta Street, where



Fig. 2. A photograph of the travelled section 6, generated based on the collected data [own study]

the data was collected, are mainly high-rise office buildings, the so-called “skyscrapers”. When the route turns into Wronia Street, the signal reception starts to be extremely disturbed. Once the measurement starts to proceed between buildings standing in proximity to each other, it ceases to have any representation in the actual course of the route. This is the measurement that is most inconsistent with reality, yet it is confirmed in theory. A signal in a place with such terrain is very often reflected, and the satellites are hidden behind the horizon. For this reason, a greater number of them are not visible.

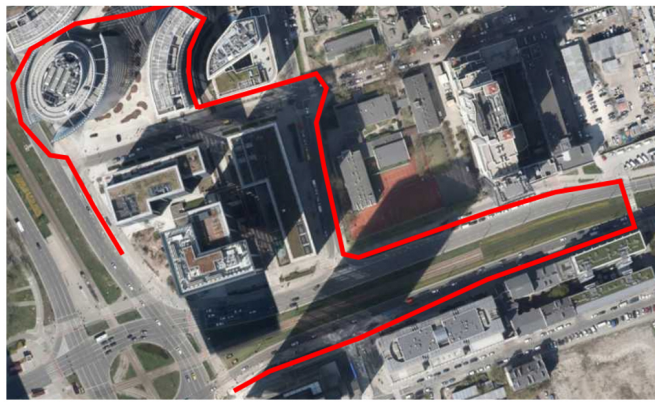


Fig. 3. The course of the route travelled during measurement No. 6 [own study]

After reconstructing the trajectory in the RTKlib program, it can be noticed that the measurement intended to be conducted on the right side of Prosta Street was directed in such a manner that it is found within the range of measurements from the return route. Actually, the trajectories of these measurements do not overlap each other at any time. Consequently, the measurement shows that the side of the street was changed twice, while it was only travelled once. In addition, the trajectory shows that the street was crossed from left to right, while in fact, the opposite was true. In no way does the measurement resemble a straight line, which does not harmonise with the factual circumstances. The greatest error was approximately 70 m.

The measurements showed that in an urban environment with high-rise buildings, it is difficult to correctly locate the companion robot. Therefore, it is necessary to use another independent system for locating the companion robot, which will not use satellite navigation systems.

4. RELIABILITY AND OPERATIONAL ANALYSIS OF A COMPANION ROBOT WITH ACCOUNT TAKEN OF THE GNSS SIGNAL MULTIPATH PROPAGATION

The concept of a companion robot involves the robot's ability to conduct a range of activities that humans do daily. It is therefore required for the companion robot to move safely in the diverse environment surrounding it (both domestic and external urban environments). The limitations on the use of a companion robot should not include the place of residence or the location of the target which could be, for example, a shop situated a few streets

away. Therefore, it is necessary to use another solution allowing the companion robot to be located, in addition to the satellite navigation system [11]. The benefit of using two navigation systems will be an increased operating range. However, the issue arises of determining the probability of a companion robot being on standby in the context of reliability and operational analysis of the double navigation system [12].

When analysing the functioning of a companion robot equipped with two navigation systems, it is possible to illustrate the relationships taking place in reliability and operational terms, as shown in Fig. 4.

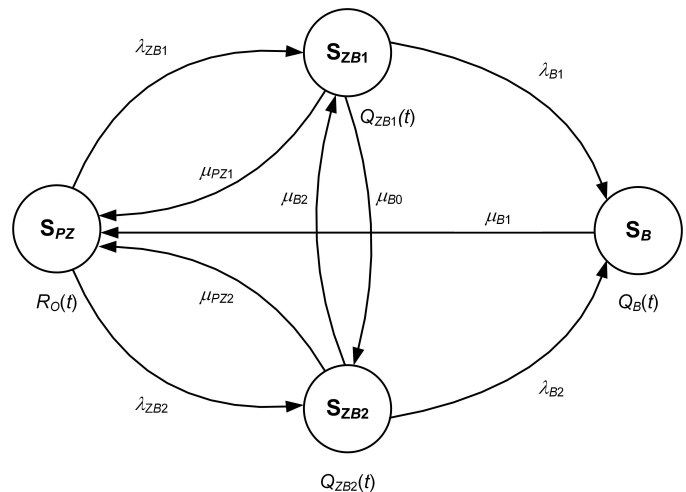


Fig. 4. Relationships in a companion robot equipped with two navigation systems [own study]

The fully fit state S_{PZ} is the state in which the companion robot functions properly. The partly fit state I S_{ZB1} is the state in which the companion robot is partly fit (GNSS navigation is fit, while LiDAR navigation is unfit). The partly fit state II S_{ZB2} is the state in which the companion robot is partly fit (GNSS navigation is unfit, while LiDAR navigation is fit). The unfit state S_B is the state in which the companion robot is unfit (both navigation systems are unfit).

If the companion robot is in the fully fit state S_{PZ} , and the LiDAR navigation gets damaged, the robot then transitions to the partly fit state I S_{ZB1} with an intensity of λ_{ZB1} . If the companion robot is in the partly fit state I S_{ZB1} , the transition to the fully fit state S_{PZ} is possible provided that activities are taken to restore the fit state.

If the partly fit state I S_{ZB1} exists, and the GNSS navigation becomes damaged, there is a transition to the unfit state S_B with an intensity of λ_{B1} .

If the companion robot is in the fully fit state S_{PZ} , and the GNSS navigation becomes damaged, the system transitions to the partly fit state II S_{ZB2} with an intensity of λ_{ZB2} . If the companion robot is in the partly fit state II S_{ZB2} , the transition to the fully fit state S_{PZ} is possible provided that activities are taken to restore the fit state.

If the partly fit state II S_{ZB2} exists, and the LiDAR navigation is damaged, there is a transition to the unfit state S_B with an intensity of λ_{B2} .

GNSS multipath error in the context of the reliability of companion robots

If the companion robot is in the partly fit state I S_{ZB1} , and there is a change in the navigation used from GNSS to LiDAR, the system transitions to the partly fit state II S_{ZB2} with an intensity of μ_{B0} .

If the companion robot is in the partly fit state II S_{ZB2} , and there is a change in the navigation used from LiDAR to GNSS, the system transitions to the partly fit state I S_{ZB1} with an intensity of μ_{B2} .

If the companion robot is in the unfit state S_B , and activities are taken to restore the fit state, the transition to the fully fit state S_{PZ} occurs with an intensity of μ_{B1} .

Designations in Fig. 4:

- $R_O(t)$ – a function of the probability of the companion robot being in a fully fit state S_{PZ} ,
- $Q_{ZB1}(t)$ – a function of the probability of the companion robot being in a partly fit state I S_{ZB1} ,
- $Q_{ZB2}(t)$ – a function of the probability of the companion robot being in a partly fit state II S_{ZB2} ,
- $Q_B(t)$ – a function of the probability of the companion robot being in an unfit state S_B ,
- λ_{ZB1} – the intensity of the transition from a fully fit state S_{PZ} to a partly fit state I S_{ZB1} ,
- λ_{ZB2} – the intensity of the transition from a fully fit state S_{PZ} to a partly fit state II S_{ZB2} ,
- μ_{PZ1} – the intensity of the transition from a partly fit state I S_{ZB1} to a fully fit state S_{PZ} ,
- μ_{PZ2} – the intensity of the transition from a partly fit state II S_{ZB2} to a fully fit state S_{PZ} ,
- μ_{B0} – the intensity of the transition from a partly fit state I S_{ZB1} to a partly fit state S_{ZB2} ,
- μ_{B2} – the intensity of the transition from a partly fit state II S_{ZB2} to a partly fit state I S_{ZB1} ,
- μ_{B1} – the intensity of the transition from an unfit state S_B to a fully fit state S_{PZ} ,
- λ_{B1} – the intensity of the transition from a partly fit state I S_{ZB1} to an unfit state S_B ,
- λ_{B2} – the intensity of the transition from a partly fit state II S_{ZB2} to an unfit state S_B .

The companion robot shown in Fig. 4 can be described using the following Kolmogorov-Smirnov equations:

$$\begin{aligned} R'_0(t) &= -\lambda_{ZB1} \cdot R_0(t) + \mu_{PZ1} \cdot Q_{ZB1}(t) - \lambda_{ZB2} \cdot R_0(t) \\ &\quad + \mu_{PZ2} \cdot Q_{ZB2}(t) + \mu_{B1} \cdot Q_B(t), \\ Q'_{ZB1}(t) &= \lambda_{ZB1} \cdot R_0(t) - \mu_{PZ1} \cdot Q_{ZB1}(t) - \lambda_{B1} \cdot Q_{ZB1}(t) \\ &\quad - \mu_{B0} \cdot Q_{ZB1}(t) + \mu_{B2} \cdot Q_{ZB2}(t), \\ Q'_{ZB2}(t) &= \lambda_{ZB2} \cdot R_0(t) - \mu_{PZ2} \cdot Q_{ZB2}(t) - \lambda_{B2} \cdot Q_{ZB2}(t) \\ &\quad + \mu_{B0} \cdot Q_{ZB1}(t) - \mu_{B2} \cdot Q_{ZB2}(t), \\ Q'_B(t) &= \lambda_{B1} \cdot Q_{ZB1}(t) + \lambda_{B2} \cdot Q_{ZB2}(t) - \mu_{B1} \cdot Q_B(t). \end{aligned} \quad (1)$$

By assuming the initial conditions:

$$\begin{aligned} R_0(0) &= 1, \\ Q_{ZB1}(0) &= Q_{ZB2}(0) = Q_B(0) = 0 \end{aligned} \quad (2)$$

and applying the Laplace transform [13], the following system of linear equations is obtained:

$$\begin{aligned} s \cdot R_0^*(s) - 1 &= -\lambda_{ZB1} \cdot R_0^*(s) + \mu_{PZ1} \cdot Q_{ZB1}^*(s) - \lambda_{ZB2} \cdot R_0^*(s) \\ &\quad + \mu_{PZ2} \cdot Q_{ZB2}^*(s) + \mu_{B1} \cdot Q_B^*(s), \\ s \cdot Q_{ZB1}^*(s) &= \lambda_{ZB1} \cdot R_0^*(s) - \mu_{PZ1} \cdot Q_{ZB1}^*(s) - \lambda_{B1} \cdot Q_{ZB1}^*(s) \\ &\quad - \mu_{B0} \cdot Q_{ZB1}^*(s) + \mu_{B2} \cdot Q_{ZB2}(t), \\ s \cdot Q_{ZB2}^*(s) &= \lambda_{ZB2} \cdot R_0^*(s) - \mu_{PZ2} \cdot Q_{ZB2}^*(s) - \lambda_{B2} \cdot Q_{ZB2}^*(s) \\ &\quad + \mu_{B0} \cdot Q_{ZB1}^*(s) - \mu_{B2} \cdot Q_{ZB2}(t), \\ s \cdot Q_B^*(s) &= \lambda_{B1} \cdot Q_{ZB1}^*(s) + \lambda_{B2} \cdot Q_{ZB2}^*(s) - \mu_{B1} \cdot Q_B^*(s). \end{aligned} \quad (3)$$

By transforming system (3), the following notation is obtained in schematic terms:

$$\begin{aligned} R_0^*(s) &= -\frac{b_1 \cdot b_2 \cdot c - c \cdot \mu_{B0} \cdot \mu_{B2}}{a \cdot c \cdot \mu_{B0} \cdot \mu_{B2} - a \cdot b_1 \cdot b_2 \cdot c + b_2 \cdot c \cdot \lambda_{ZB1} \cdot \mu_{PZ1}} \\ &\quad + b_1 \cdot c \cdot \lambda_{ZB2} \cdot \mu_{PZ2} + b_2 \cdot \lambda_{B1} \cdot \mu_{B1} \cdot \lambda_{ZB1} \\ &\quad + b_1 \cdot \lambda_{B2} \cdot \mu_{B1} \cdot \lambda_{ZB2} + c \cdot \mu_{B0} \cdot \lambda_{ZB1} \cdot \mu_{PZ2} \\ &\quad + c \cdot \mu_{B2} \cdot \mu_{PZ1} \cdot \lambda_{ZB2} + \mu_{B0} \cdot \lambda_{B2} \cdot \mu_{B1} \cdot \lambda_{ZB1} \\ &\quad + \lambda_{B1} \cdot \mu_{B1} \cdot \mu_{B2} \cdot \lambda_{ZB2} \\ Q_{ZB1}^*(s) &= -\frac{b_2 \cdot c \cdot \lambda_{ZB1} + c \cdot \mu_{B2} \cdot \lambda_{ZB2}}{a \cdot c \cdot \mu_{B0} \cdot \mu_{B2} - a \cdot b_1 \cdot b_2 \cdot c + b_2 \cdot c \cdot \lambda_{ZB1} \cdot \mu_{PZ1}} \\ &\quad + b_1 \cdot c \cdot \lambda_{ZB2} \cdot \mu_{PZ2} + b_2 \cdot \lambda_{B1} \cdot \mu_{B1} \cdot \lambda_{ZB1} \\ &\quad + b_1 \cdot \lambda_{B2} \cdot \mu_{B1} \cdot \lambda_{ZB2} + c \cdot \mu_{B0} \cdot \lambda_{ZB1} \cdot \mu_{PZ2} \\ &\quad + c \cdot \mu_{B2} \cdot \mu_{PZ1} \cdot \lambda_{ZB2} + \mu_{B0} \cdot \lambda_{B2} \cdot \mu_{B1} \cdot \lambda_{ZB1} \\ &\quad + \lambda_{B1} \cdot \mu_{B1} \cdot \mu_{B2} \cdot \lambda_{ZB2} \\ Q_{ZB2}^*(s) &= -\frac{b_1 \cdot c \cdot \lambda_{ZB2} + c \cdot \mu_{B0} \cdot \lambda_{ZB1}}{a \cdot c \cdot \mu_{B0} \cdot \mu_{B2} - a \cdot b_1 \cdot b_2 \cdot c + b_2 \cdot c \cdot \lambda_{ZB1} \cdot \mu_{PZ1}} \\ &\quad + b_1 \cdot c \cdot \lambda_{ZB2} \cdot \mu_{PZ2} + b_2 \cdot \lambda_{B1} \cdot \mu_{B1} \cdot \lambda_{ZB1} \\ &\quad + b_1 \cdot \lambda_{B2} \cdot \mu_{B1} \cdot \lambda_{ZB2} + c \cdot \mu_{B0} \cdot \lambda_{ZB1} \cdot \mu_{PZ2} \\ &\quad + c \cdot \mu_{B2} \cdot \mu_{PZ1} \cdot \lambda_{ZB2} + \mu_{B0} \cdot \lambda_{B2} \cdot \mu_{B1} \cdot \lambda_{ZB1} \\ &\quad + \lambda_{B1} \cdot \mu_{B1} \cdot \mu_{B2} \cdot \lambda_{ZB2} \\ Q_B^*(s) &= -\frac{b_2 \cdot \lambda_{B1} \cdot \lambda_{ZB1} + b_1 \cdot \lambda_{B2} \cdot \lambda_{ZB2}}{a \cdot c \cdot \mu_{B0} \cdot \mu_{B2} - a \cdot b_1 \cdot b_2 \cdot c + b_2 \cdot c \cdot \lambda_{ZB1} \cdot \mu_{PZ1}} \\ &\quad + \mu_{B0} \cdot \lambda_{B2} \cdot \lambda_{ZB1} + \lambda_{B1} \cdot \mu_{B2} \cdot \lambda_{ZB2} \\ &\quad + b_1 \cdot c \cdot \lambda_{ZB2} \cdot \mu_{PZ2} + b_2 \cdot \lambda_{B1} \cdot \mu_{B1} \cdot \lambda_{ZB1} \\ &\quad + b_1 \cdot \lambda_{B2} \cdot \mu_{B1} \cdot \lambda_{ZB2} + c \cdot \mu_{B0} \cdot \lambda_{ZB1} \cdot \mu_{PZ2} \\ &\quad + c \cdot \mu_{B2} \cdot \mu_{PZ1} \cdot \lambda_{ZB2} + \mu_{B0} \cdot \lambda_{B2} \cdot \mu_{B1} \cdot \lambda_{ZB1} \\ &\quad + \lambda_{B1} \cdot \mu_{B1} \cdot \mu_{B2} \cdot \lambda_{ZB2} \end{aligned} \quad (4)$$

where:

$$\begin{aligned} a &= s + \lambda_{ZB1} + \lambda_{ZB2}, \\ b_1 &= s + \mu_{PZ1} + \lambda_{B1} + \mu_{B0}, \\ b_2 &= s + \mu_{PZ2} + \lambda_{B2} + \mu_{B2}, \\ c &= s + \mu_{B1}. \end{aligned} \quad (5)$$

By conducting further mathematical analysis (4) and (5), relationships are obtained that facilitate computing the values of the probabilities of the companion robot in the following states: fully fit state S_{PZ} , partly fit state I S_{ZB1} , partly fit state II S_{ZB2} , and the unfit state S_B .

5. MODELLING THE COMPANION ROBOT OPERATION PROCESS

By using computer assistance and equations (4) and (5), computations can be performed to enable the determination of the value of the probability of the companion robot being in the operational states adopted for the analysis. This is illustrated in the following example.

Example:

Let us assume [14] the following values describing the companion robot under analysis:

- The duration of research – 1 year (the value of the duration is provided in the hour units [h]):

$$t = 8760 \text{ [h].}$$

- The intensity of the companion robot transition from a fully fit state to a partly fit state I λ_{ZB1} :

$$\lambda_{ZB1} = 0.000001 \text{ [1/h].}$$

- The intensity of the companion robot transition from a fully fit state to a partly fit state II λ_{ZB2} :

$$\lambda_{ZB2} = 0.0000001 \text{ [1/h].}$$

- The intensity of the companion robot transition from a partly fit state I to an unfit state λ_{B1} :

$$\lambda_{B1} = 0.0000001 \text{ [1/h].}$$

- The intensity of the companion robot transition from a partly fit state II to an unfit state λ_{B2} :

$$\lambda_{B2} = 0.000001 \text{ [1/h].}$$

- The intensity of the companion robot transition from a partly fit state I to a partly fit state II μ_{B0} :

$$\mu_{B0} = 0.00000001 \text{ [1/h].}$$

- The intensity of the companion robot transition from a partly fit state II to a partly fit state I μ_{B2} :

$$\mu_{B2} = 0.00000001 \text{ [1/h].}$$

- The intensity of the companion robot transition from an unfit state to a fully fit state μ_{B1} :

$$\mu_{B1} = 0.01 \text{ [1/h].}$$

- The intensity of the companion robot transition from a partly fit state I to a fully fit state μ_{PZ1} :

$$\mu_{PZ1} = 0.1 \text{ [1/h].}$$

- The intensity of the companion robot transition from a partly fit state II to a fully fit state μ_{PZ2} :

$$\mu_{PZ2} = 0.2 \text{ [1/h].}$$

The above numerical values were adopted based on the results of observations of the operation process of electronic devices used in navigation systems [15]. Reliability and operational analyses from the field of navigation systems used in transport were also used [16].

For the above input values, using equations (4) and (5), the following is obtained:

$$R_0^*(s) = \frac{5.5000454 \cdot 10^{16} \cdot s + 5.05 \cdot 10^{16} \cdot \mu_{PZ1} + 4.5 \cdot 10^{15} \cdot \mu_{PZ2} + 5 \cdot 10^{24} \cdot s^2 \cdot \mu_{PZ1} + 5 \cdot 10^{24} \cdot s^2 \cdot \mu_{PZ2} + 5.00055 \cdot 10^{22} \cdot s^2 + 5 \cdot 10^{24} \cdot s^3 + 5.000505 \cdot 10^{22} \cdot s \cdot \mu_{PZ1} + 5.000045 \cdot 10^{22} \cdot s \cdot \mu_{PZ2} + 5 \cdot 10^{22} \cdot \mu_{PZ1} \cdot \mu_{PZ2} + 5 \cdot 10^{24} \cdot s \cdot \mu_{PZ1} \cdot \mu_{PZ2} + 4.54 \cdot 10^9}{5.50404994 \cdot 10^{10} \cdot s - 1 \cdot 10^9 \cdot \mu_{PZ2} + 5.000555 \cdot 10^{22} \cdot s^2 \cdot \mu_{PZ1} + 5.000545 \cdot 10^{22} \cdot s^2 \cdot \mu_{PZ2} + 5 \cdot 10^{24} \cdot s^3 \cdot \mu_{PZ1} + 5 \cdot 10^{24} \cdot s^3 \cdot \mu_{PZ2} + 1.10006504 \cdot 10^{17} \cdot s^2 + 5.0011 \cdot 10^{22} \cdot s^3 + 5 \cdot 10^{24} \cdot s^4 + 5.55005 \cdot 10^{16} \cdot s \cdot \mu_{PZ1} + 5.45004 \cdot 10^{16} \cdot s \cdot \mu_{PZ2} + 5 \cdot 10^{22} \cdot s \cdot \mu_{PZ1} \cdot \mu_{PZ2} + 5 \cdot 10^{24} \cdot s^2 \cdot \mu_{PZ1} \cdot \mu_{PZ2} - 1011} \quad (6)$$

Relationship (6) determines the probability of the companion robot being in a fully fit state in symbolic (Laplace) terms.

As a result of the transformations, the following are obtained:

$$R_0(t) = 1.63738547 \cdot 10^{-10} \cdot e^{-0.01 \cdot t} + 5.00004043 \cdot 10^{-7} \cdot e^{-0.2000011 \cdot t} + 0.00000999986 \cdot e^{-0.10000108 \cdot t} + 0.99998949996 \cdot e^{1.9999772 \cdot 10^{-13} \cdot t}. \quad (7)$$

Relationship (7) determines the probability of the companion robot being in a fully fit state in the time domain.

As the final result, the following is obtained:

$$R_O(8760) = 0.9999895. \quad (8)$$

Result (8) determines the probability of the companion robot being in a fully fit state for time $t = 8760$ [h] (i.e., after one year of exploitation).

The obtained value of the probability of the companion robot being in a fully fit state, in terms of the navigation solutions used, is sufficient for non-commercial applications. However, further research should also consider aspects related to maintenance activities (including periodic inspections and e-maintenance).

The presented reliability and operational analysis of the companion robot allows designers to make decisions regarding the

selection of individual navigation systems to rationalise the values of the probabilities of the robot being in the designated states (particularly in the fully fit state).

6. CONCLUSIONS

A companion robot is a device adapted to perform various tasks to assist humans (in particular the elderly and people with disabilities). For this to be possible, not only must the robot be capable of communicating with its surroundings, but it must be able to move safely in an autonomous manner.

The study demonstrated that the use of a companion robot in an urban environment with tall buildings is hindered, which is related to the multipath propagation of the global navigation satellite signal. To increase the accuracy of the location of the companion robot and thus increase the safety of the activities being taken, it is beneficial to apply the second solution that facilitates the determination of the location of the companion robot. The study conducted a reliability and operational analysis of the companion robot in which two navigation solutions were applied. Relationships were established to compute the values of the probabilities of a companion robot being in specific functional states. Therefore, it is possible to use the presented considerations to compare diverse types of solutions applied in a companion robot in navigational terms and select a reasonable one that will enable the performance of the intended activities in a specific external environment. The analysed solutions were as follows: LIDAR technique, GNSS, and TDoA. It can be seen that the LIDAR technique gives the best results in terms of positioning accuracy and adaptation in a diverse environment. GNSS works best in terms of navigation range and wide availability. In turn, TDoA is best when available inside buildings and is the most cost-efficient solution.

In further research, the authors are planning to consider sensors used in the companion robot, which enable the determination of the position thanks to markers placed at designated points of the urban canyons.

FUNDING

Research work was financed by the state budget under the program of the Minister of Education and Science (POLAND), called "Science for Society" project number Nds/536964/2021/2021 amount of funding PLN 1 557 100. Total value of the project PLN 1 557 100.

REFERENCES

- [1] M. Maroto-Gómez, F. Alonso-Martín, M. Malfaz, A. Castro-González, J.C. Castillo, and M.A. Salichs, "A Systematic Literature Review of Decision-Making and Control Systems for Autonomous and Social Robots," *Int. J. Soc. Robot.*, vol. 15, pp. 745–789, 2023, doi: [10.1007/s12369-023-00977-3](https://doi.org/10.1007/s12369-023-00977-3).
- [2] M. Takada, J. Ichino, and K. Hayashi, "A Study of Objective Evaluation Indicator Based on Robot Activity Logs for Owner Attachment to Companion Robot," *Int. J. Soc. Robot.*, vol. 16, pp. 125–143, 2023, doi: [10.1007/s12369-023-01030-z](https://doi.org/10.1007/s12369-023-01030-z).
- [3] T. Kanda, "Enabling Harmonized Human-Robot Interaction in a Public Space," in *Human-Harmonized Information Technology*, T. Nishida, Ed., Tokyo: Springer, 2017, pp. 115–137, doi: [10.1007/978-4-431-56535-2_4](https://doi.org/10.1007/978-4-431-56535-2_4).
- [4] K. Krzykowska-Piotrowska, E. Dudek, M. Siergiejczyk, A. Rosiński, and W. Wawryński, "Is Secure Communication in the R2I (Robot-to-Infrastructure) Model Possible? Identification of Threats," *Energies*, vol. 14, no. 15, p. 4702, Aug. 2021, doi: [10.3390/en14154702](https://doi.org/10.3390/en14154702).
- [5] S. Herbster, R. Behrens, and N. Elkmann, "Modeling the Contact Force in Constrained Human–Robot Collisions," *Machines*, vol. 11, no. 10, p. 955, Oct. 2023, doi: [10.3390/machines11100955](https://doi.org/10.3390/machines11100955).
- [6] K. Chwedczuk *et al.*, "Izzivi pri določanju višin gorskih vrhov, kot so navedene v kartografskih virih. (Challenges related to the determination of altitudes of mountain peaks presented on cartographic sources)," *Geod. Vestn.*, vol. 66, no. 1, p. 49–59, 2022, doi: [10.15292/geodetski-vestnik.2022.01.49-59](https://doi.org/10.15292/geodetski-vestnik.2022.01.49-59).
- [7] K. Krzykowska-Piotrowska, *Forecasting satellite navigation signal in civil aviation*, Warsaw: Publishing House of the Warsaw University of Technology, 2020.
- [8] X. Ji, Q. Zhu, J. Wang, C. Cai, and J. Ma, "Mobile robot visual homing by vector pre-assigned mechanism", *Bull. Pol. Acad. Sci. Tech. Sci.*, vol. 67, no. 2, pp. 213–227, 2019, doi: [10.24425/bpas.2019.128114](https://doi.org/10.24425/bpas.2019.128114).
- [9] K. Krzykowska-Piotrowska, E. Dudek, P. Wielgosz, B. Milanowska, and J.M. Batalla, "On the Correlation of Solar Activity and Troposphere on the GNSS/EGNOS Integrity. Fuzzy Logic Approach," *Energies*, vol. 14, no. 15, p. 4534, Jul. 2021, doi: [10.3390/en14154534](https://doi.org/10.3390/en14154534).
- [10] R. Halili, M. Weyn, and R. Berkvens, "Comparing Localization Performance of IEEE 802.11p and LTE-V V2I Communications," *Sensors*, vol. 21, no. 6, p. 2031, Mar. 2021, doi: [10.3390/s21062031](https://doi.org/10.3390/s21062031).
- [11] K. Krasuski, J. Ćwiklak, M. Bauka, and M. Mrozik, "Analysis of the Determination of the Accuracy Parameter for Dual Receivers Based on EGNOS Solution in Aerial Navigation," *Acta Mech. Automatica*, vol 16, no. 4, pp. 365–372, 2022, doi: [10.2478/ama-2022-0043](https://doi.org/10.2478/ama-2022-0043).
- [12] N. Li, L. Zhao, L. Li, and C. Jia, "Integrity monitoring of high-accuracy GNSS-based attitude determination," *GPS Solut.*, vol. 22, p. 120, 2018, doi: [10.1007/s10291-018-0787-x](https://doi.org/10.1007/s10291-018-0787-x).
- [13] F. Grabski, *Semi-Markov Processes: Applications in System Reliability and Maintenance*, Amsterdam: Elsevier, 2015, doi: [10.1016/C2013-0-14260-2](https://doi.org/10.1016/C2013-0-14260-2).
- [14] J. Paś and S. Buchla, "Exploitation of Electronic Devices - Selected Issues," *J. KONBiN*, vol. 49, no. 1, pp. 125–142, 2019, doi: [10.2478/jok-2019-0007](https://doi.org/10.2478/jok-2019-0007).
- [15] F. Zangenehnejad and Y. Gao, "GNSS smartphones positioning: advances, challenges, opportunities, and future perspectives," *Satell. Navig.*, vol. 2, p. 24, 2021, doi: [10.1186/s43020-021-00054-y](https://doi.org/10.1186/s43020-021-00054-y).
- [16] M. Rychlicki, Z. Kasprzyk, and A. Rosiński, "Analysis of Accuracy and Reliability of Different Types of GPS Receivers," *Sensors*, vol. 20, no. 22, p. 6498, Nov. 2020, doi: [10.3390/s20226498](https://doi.org/10.3390/s20226498).